ISSN: 0067-2904

Influence of Dielectric Media on the Plasma Characteristics in DBD Discharge

Sarah Faris Khaleel*, Qusay A. Abbas
Department of Physics, College of Science, University of Baghdad, Baghdad, Iraq

Received: 4/4/2021 Accepted: 8/8/2021 Published: 30/6/2022

Abstract

The study of the surface plasma characteristics under atmospheric pressure is a new branch and tool in physics. Building generation dielectric barrier discharge (DBD) system at atmospheric pressure and studying its thermal characterizations. The discharge was produced by applying a high voltage of 20 kV with a frequency of 8 kHz. The thermal characterization was done by measuring discharge temperature for different horizontal surface areas and different types of insulating material. The results indicated that the effect of the area and the type of insulator affect the discharge (increasing or decreasing) according to the operation conditions because they affect, as expected, the DBD . The plasma temperature increased with the decrease of the surface area, which resulted in the increase of the discharge voltage across the gap; accordingly, the discharge across the gap grew.

Keywords: DBD, Boltzmann plot method, stark broadening, Electron temperature.

تأثير الوسائط العازلة على خاصية البلازما في تفريغ الحاجز العازل

ساره فارس خليل*, قصي عدنان عباس
قسم الفيزياء, كلية العلوم, جامعة بغداد، بغداد، العراق

الخلاصة

خصائص البلازما السطحية للضغط الجوي هي فرع جديد وأداة في الفيزياء ، بناء نظام تصريف حاجز عازل (DBD) عند الضغط الجوي ودراسة خصائصه الحرارية. تم إنتاج التفريغ باستخدام جهد عالي 20 كيلو فولت وتردد 8 كيلو هرتز. تم إجراء التوصيف الحراري عن طريق قياس درجة حرارة التفريغ عند تغيير مساحة السطح الأفقية ونوع المادة العازلة. تشير النتائج إلى أن تأثير المساحة ونوع العزل يؤثران على التصريف (زيادة أو نقصان) وفقًا لظروف التشغيل لأنها تؤثر ، كما هو متوقع ، على زيادة درجة حرارة بلازما DBD مع تناقص مساحة السطح مما يؤدي إلى زيادة جهد التفريغ عبر الفجوة ، وفقًا لذلك ، ينمو التفريغ عبر الفجوة أيضًا.

1. Introduction

The electrical discharge between two electrodes separated by an insulating dielectric barrier is called dielectric-barrier discharge (DBD)[1]. Volume or vertical discharge and

*Email: sarah.khaleel1204@sc.uobaghdad.edu.iq

surface discharge are the two different types of DBD. Glass, quartz, ceramics, epoxy, and enamels are popular dielectric barrier materials. Other components that can be used include acrylic films, silicon rubber, Teflon covers, etc. Werner Von Siemens announced the first scientific investigation for ozone production in 1857 [2]. DBDs have been used to enhance wet ability, printability, and adhesion in polymer surfaces. The dielectric barrier discharge (DBD) has a range of potential industrial applications and has been a research focus for many years[3]. It has the ability to improve surface processing at ambient pressure and plasma chemistry. The most critical feature of DBD is that it is much easier to maintain a non-thermal equilibrium plasma state than other methods such as low-pressure discharges, fast-pulsed high-pressure discharges, or electron beam injection. The flexibility with respect to geometrical configuration, operating parameters, and operating medium is another important benefit of atmospheric pressure DBD [4]. Polymers are products made up of long, repeated molecule strings. The properties of the materials vary based on the form of the bound molecules and how they are bonded. Rubber and polyester are examples of polymers that bend and stretch. Others, such as epoxies and glass, are rough and rugged [5].

Single dielectric barrier discharge (SDBD) plasma actuator, a modern flow control method that has the ability to do this, has recently been investigated. For the past decade, these have been thoroughly researched ([6] , [7] and[8]). A typical SDBD system has two electrodes offset in the chordwise direction and separated by a dielectric plate, usually Kapton, glass, quartz, or ceramics. The exposed electrode is connected to a high voltage source, while the encapsulated electrode is grounded. Typically, the required voltages are in the kV range, with frequency in the kHz range. As the device is turned on, a purplish light plasma appears, which begins at the exposed electrode and spreads over the dielectric surface above the encapsulated electrode. The plasma is ionized air consisting of electrons and ions with the bulk plasma exhibiting electrical neutrality. This arrangement can create a steady jet that flows away from the exposed electrode over to the encapsulated electrode on a seconds-scale without any moving parts. The plasma actuator is small, lightweight, repairable, flexible, and can follow the curvature of the surface. It has a high frequency response and can be turned on, off with the flip of a button. It can be triggered at a broad range of modulation frequencies([9],[10]). Several studies have shown that discharges in air under atmospheric pressure may be used for plasma treatment of polymers for surface and adhesion improvement. Hegemann et al. [11] studied different plasma treatments in rf discharge of Ar, He, or N_2, cross-link, and activate polymers like PC, PP, EPDM, PE, PS, PET and PMMA. Saleh et al. [12] designed a dielectric barrier discharge (DBD) plasma system. They used glass as a dielectric barrier. Non-thermal DBD Plasma was produced by applying AC voltage between the two electrodes and a glass plate as the dielectric barrier. The effect of electrodes type on the properties of produced DBD Plasma was studied. Teșoi et al. [13] investigated how plasma treatment of polymeric surfaces alters surface properties without affecting internal properties. The goal was to investigate the effects of DBD plasma on various polymeric surfaces to develop their printing capability.

In this work, the effect of surface area change and the effect of the type of insulator on the DBD plasma characteristic under atmospheric pressure were studied.

2. Experimental part

The designed DBD system consists of two aluminium electrodes with an insulator between them with different horizontal opposite area. The electrodes, with dimensions of 25.4x76.2mm, were placed inside Teflon, connected to an AC power supply. The applied AC voltage was up to 20 kV at a frequency of 8 kHz. The distance between the two electrodes was 7 mm and the thickness of the insulating material was 3 mm.

Two types of insulators(dielectric) were used. The first was pure epoxy((Euxit 50 KI)) which was transformed into a solid by combining it with a hardener (Euxit 50 KII) at a ratio of(1:3)[14]. The second was conductor epoxy which is epoxy mixed with copper at a mixing ratio of 1%.
Plasma was formed on the surface of the insulator. Thorlabs compact spectrometer (Type CCS 100/M, made in Germany)was used to determine the emitted wavelengths of the light produced by the induced plasma collected with an optical fibre. The spectrometer used has high resolution depending on the grating used and responds to a wavelength between (320 – 740) nm with resolution $\Delta\lambda < 0.5nm$, Slit: 20µm.
Figure 1 shows the DBD system.

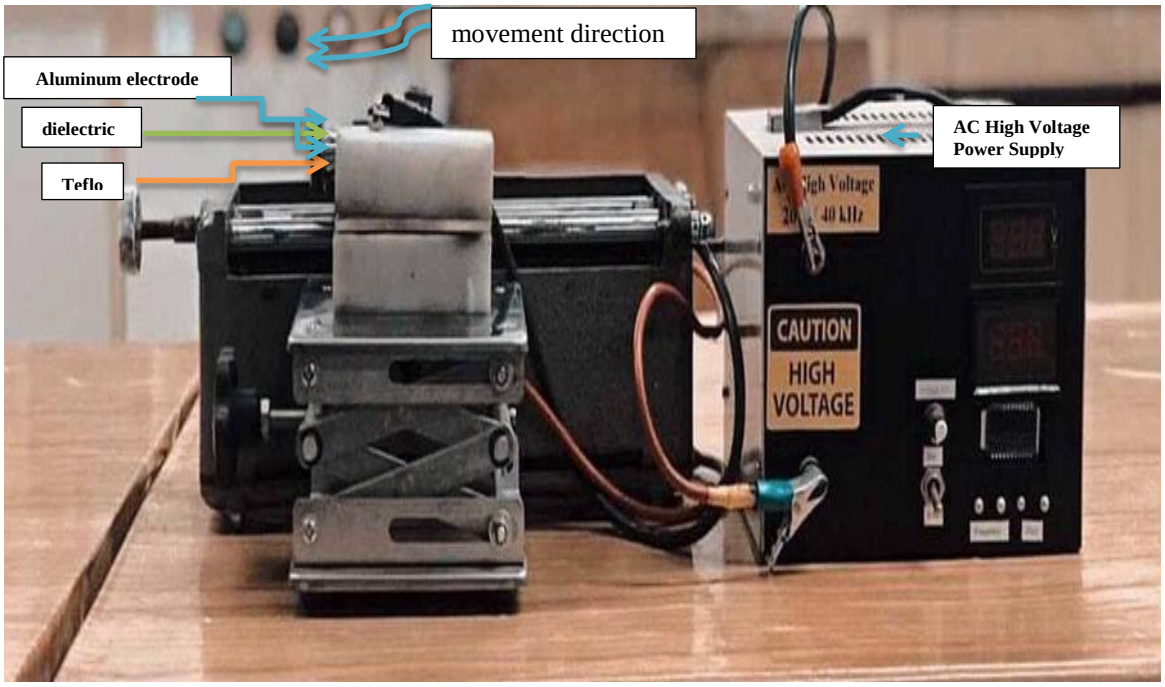

Figure 1- the DBD system.

3. Results and discussions

3.1 plasma emission spectra

3.1.1 Using epoxy resin as the dielectric

Using the optical emission spectroscopy (OES) technique, the spectroscopic emission patterns of DBD plasma, recorded in the spectral range of (320 –740) nm, at air under atmospheric pressure, using pure epoxy dielectric with 7 mm inter-electrode distance and an applied voltage of 20 kV and 8 kHz frequency are shown in Figure 2 for different horizontal opposite area.These were compared with the atomic and ionic lines for nitrogen (NI, NII) [17], in addition to the molecular lines for N_2 and N_2+ gas[15]. There are many N_2 molecular peaks in the range from 320 to 440 nm and some peaks corresponding to atomic lines NI (493 .5), NI(496.398), NI(648.27), NI(664.496). In all samples, the peak intensities are seen to decrease with the increase of the electrodes horizontal surface area.This decrease results from the optical fiber dimension due to the actuator. The identification of a plasma emission line is essential since it is the first step in determining the charge states of plasma species.

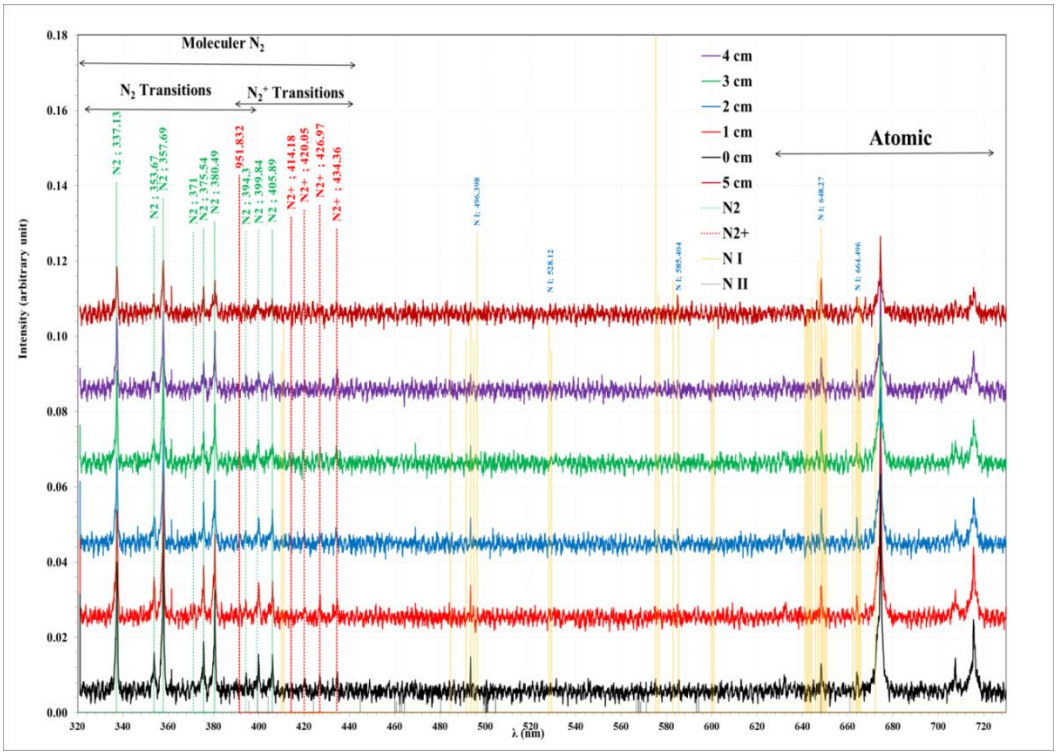

Figure 2-The plasma spectra produced for different distances with pure epoxy as the dielectric.

Figure-3 focuses on the range of the N_2 molecular lines, between 320 to 440 nm, to distinct the peaks corresponding to the transition between molecular energy levels, when the inter electrode distance is 7 cm. The figure shows many peaks corresponding to $\pi - \pi^*$ transitions indicated by red color and others for $\sigma - \sigma^*$ transitions for nitrogen molecular transition. These transitions are not pure electronic transitions but with additional energy for vibrational and rotational energies depending on the difference between vibrational quantum number of upper and lower energies for this transition. The peaks indicated with (0-0) sign refer to transition between two electronic levels but with the same vibrational quantum number (v=0 and $\acute{v}$ = 0), i.e. pure electronic transition, located at 336.6 nm for $\pi - \pi^*$ and at 391.4 for $\sigma - \sigma^*$ from which the energy difference between these electronic levels can be calculated, which are 3.684 and 3.168 eV, respectively. The other lines corresponding to Δv=-1, -2 and -3 were shifted to lower energy (longer wavelength) with energy equal to multiple the energy difference between the vibrational levels (about 0.211 eV), which is much less than the electronic energy difference. The levels split into two or three sub levels due to variation in energy differences between the vibrational levels due to coupling with rotational energy levels. It can be noticed that the emission peaks intensity increases with increasing the applied voltage due to the increase of the energy delivered to the electrons which may excite more molecules and atoms by collision.

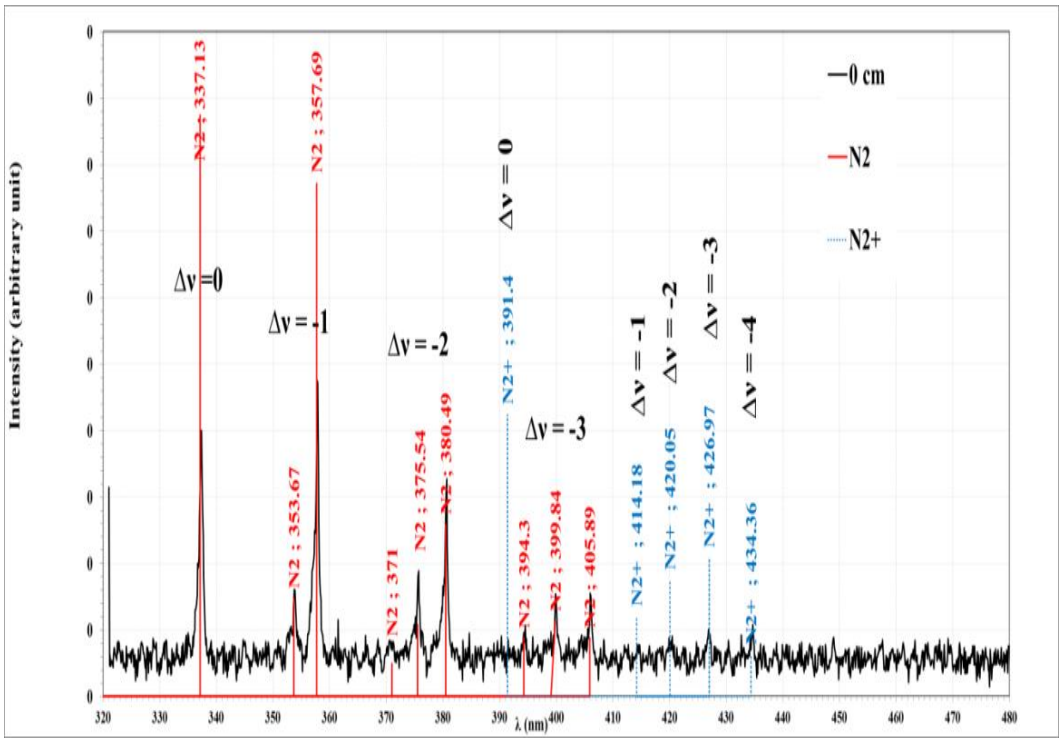

Figure 3-The plasma emission pattern for epoxy dielectric compared with N2 molecular lines at 330 – 440 nm wavelength range.

Figure 4 shows the variation of peaks intensities for the pure electronic transitions (λ= 380.49nm , 357.69 nm and 337.13 nm). This figure shows that the peaks intensities for 357.69 nm are higher than that for 380.49nm and 337.13 nm due to the difference in probability of transitions between them. The intensity of the spectrum decreases with the increase of the horizontal distance i.e. decrease of the area between the electrodes, causing the decrease of plasma diffusion, hence the decrease of intensity.

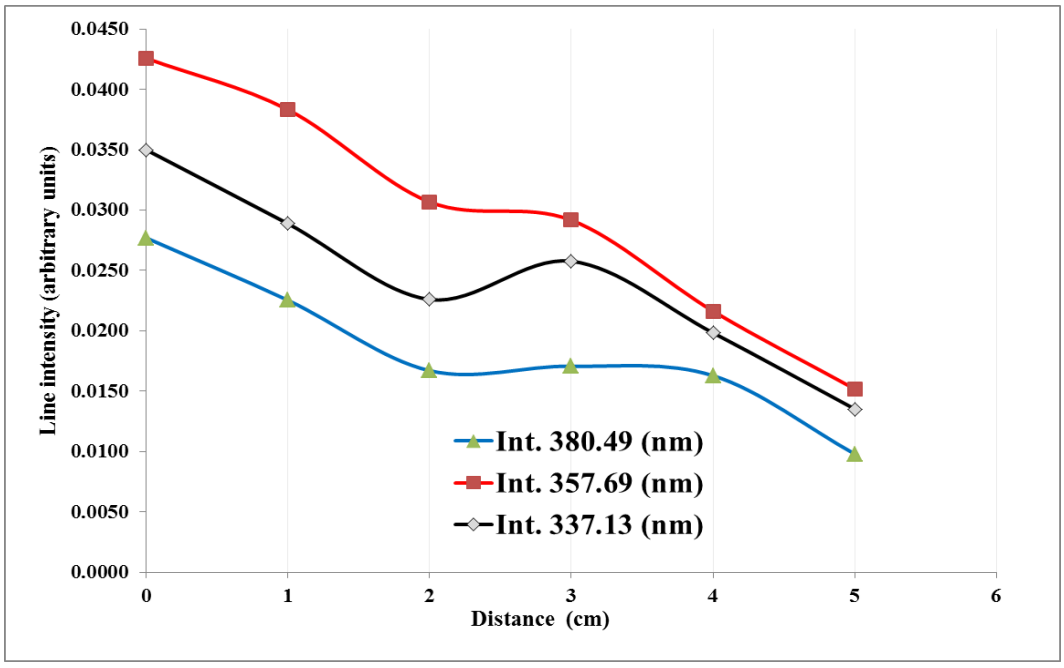

Figure 4-Variation of the maximum line intensities for pure electronic transition with different horizontal distance for pure epoxy as the dielectric.

3.1.1 Using epoxy-copper the dielectric

Figures 5 shows the stimulated emission and measured spectra of molecular nitrogen with epoxy-copper dielectric, in air at different distance using optical emission spectroscopy (OES) technique. The emission spectra were recorded in the spectral range of (320-740) nm. There are many N_2 molecular peaks in the range from 320 to 440 nm and some peaks corresponding to atomic lines NI (493.51), NI (496.40), NI (528.12), NI (648.27), and NI (664.50), in all samples. The intensities of the peaks can be seen to decrease with the horizontal surface area of the electrodes. This decrease is as a result of the optical fiber dimension due to the actuator.

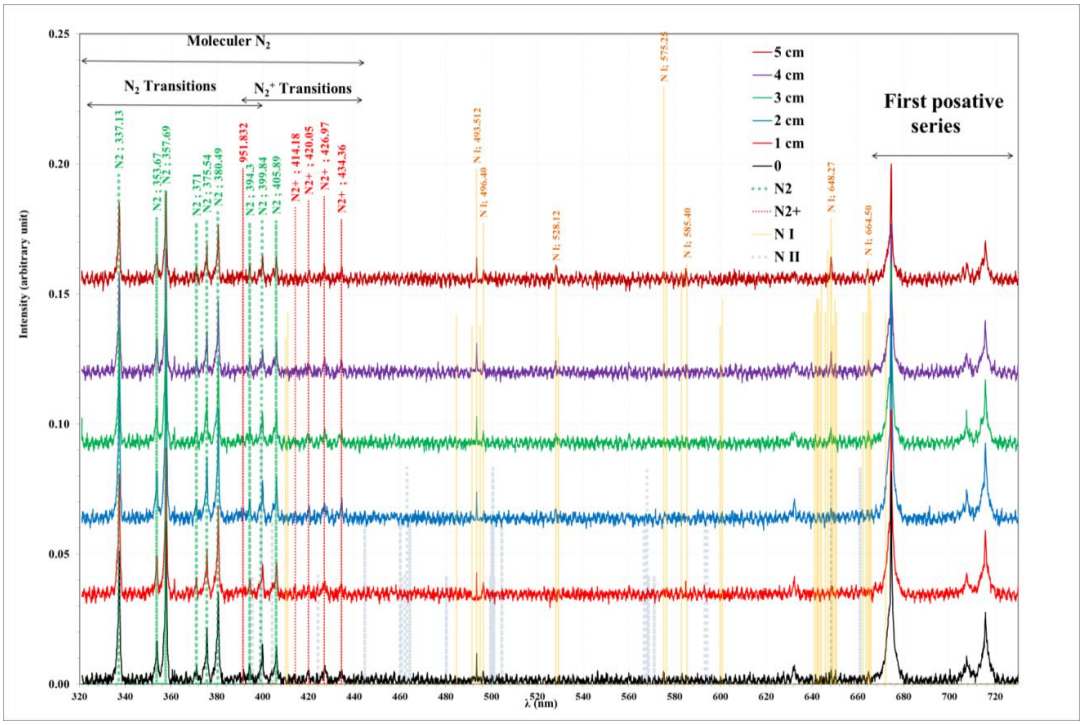

Figure 5-The plasma spectrum produced by changing the interelectrode distance with epoxy-copper dielectric.

Figures 6 shows the variation of peaks intensities for the pure electronic transitions (λ= 380.49nm, 357.69 nm, and 337.13 nm). This figure shows that all peaks intensities for 357.69 nm are higher than that for 380.49nm and 337.13 nm. This is due to the difference in their probability of transitions. There is a gradual rise of the plasma spectrum when moving the electrode in a horizontal direction at 2 cm, and then it decreases as the surface area decreases. This means that the highest plasma diffusion, when using epoxy-copper as the dielectric, occurs at the electrode displacement of 2 cm.

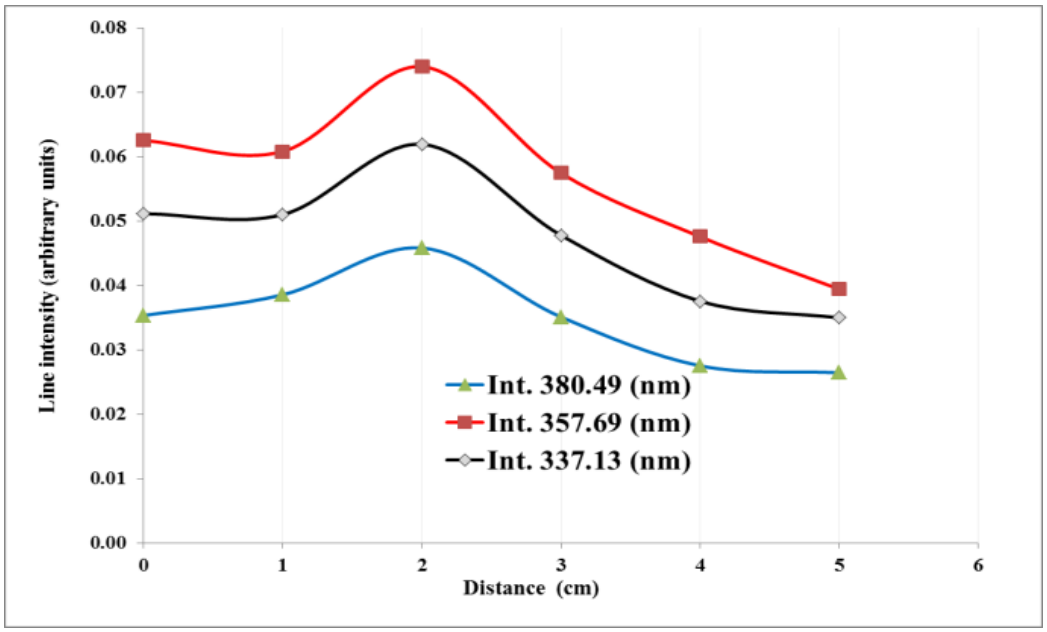

Figure 6- Variation of the maximum line intensity for pure electronic transition with different horizontal distances with epoxy-copper dielectric.

Figures 7 displays the variation of vibrational temperature ($T_{Vib.}$) with pure epoxy and with epoxy-copper dielectrics. For the pure epoxy dielectric, there is an increase in the vibration temperature with the increase of inter-electode distance (decreasing horizontal surface area) to a maximum at 3 cm distance, then a decrease in the vibration temperature as the corresponding surface area of the electrodes decreases. As for the epoxy-copper (conductive epoxy) dielectric, there is a gradual increase in the vibration temperature to a cm, and then a gradual decrease of the vibration temperature. This means that the maximum gas flow rate under atmospheric pressure occurs at 3 cm inter-electrode distance. The T_{vib} values increases as the gas flow rate increases.

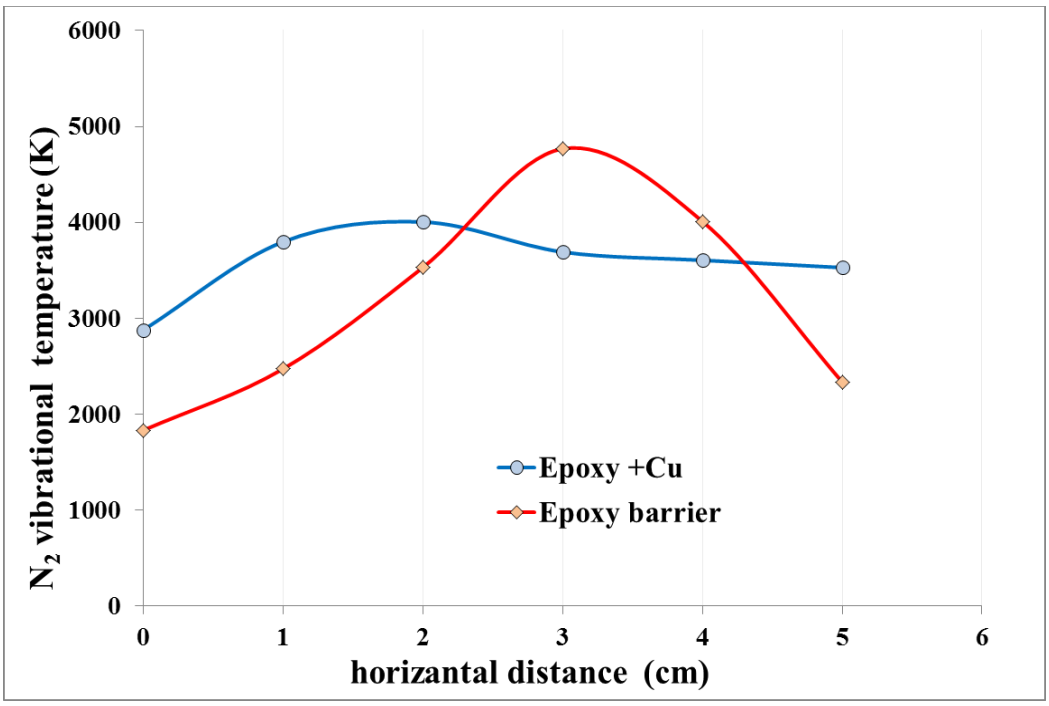

Figure 7- Variation of vibrational temperature with distance change.

3.2 plasma characteristics

3.2.1 With pure epoxy dielectric

The Boltzmann plots require tops that originate from the same atomic species and the same ionization stage. For epoxy dielectric in air, as shown in Figure 8, the slope of the fitted line is equal to (-1/ T_e). R^2 is a mathematical coefficient that indicates the goodness of a linear fit with a range of values between 0 and 1. For each fitting equation in the spectral range fitting line and R^2 were shown in Figure 8. The one that is higher has a R value that is closer to 1.

$$\ln\left(\frac{I\lambda}{A_{Ki}g_K}\right) = -\frac{E_K}{K_\beta T_e} + C \quad (1)$$

I is the intensity of a spectral line that corresponds to the change between atomic species levels Ek and Ei, λ represents wavelength, $A_{Ki}$is the probability of a transition, K is Boltzmann constant, E_k is excited level energy, g_k is statistical weight for the upper level, T_e is the electron temperature [16].

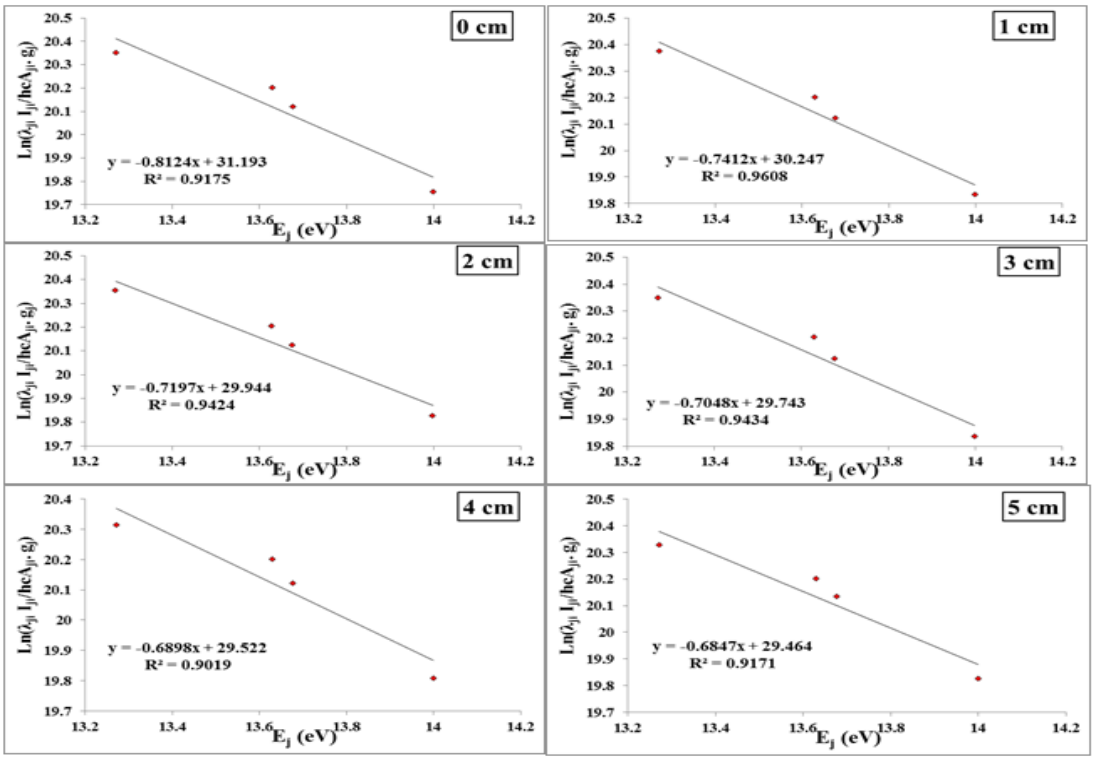

Figure 8-Boltzmann plots of pure epoxy with different distance in air.

The electron temperatures (T_e) determined using the Boltzmann plots equations indicated that the electron temperature (T_e) and the electron density (n_e) increased with the decrease of the electrodes surface area in the air. This is due to the increase of surface plasma density, as shown in Figure 9.

$$n_e \approx \left(\frac{\Delta\lambda_{FWHM}}{2.\omega_s}\right).N_r \quad (2)$$

Where: $\Delta\boldsymbol{\lambda}_{FWHM}$ is fundamental width at half maximum of measured line, ω_s is the Stark broadening parameter, N_r = 10^{16} for neutral or 10^{17} for ionic [16]. Figure 9 shows the 493.5 nm using Lorentzian fitting to find the full width at half limit (Δλ), which was used to quantify the electron density at various distances using the Stark effect based on the usual broadening values for this line (ω_m = 0.155 Å for peak λ=493.5nm) [17]. It can be seen that the full width increases with a decrease in the surface area of the electrodes.

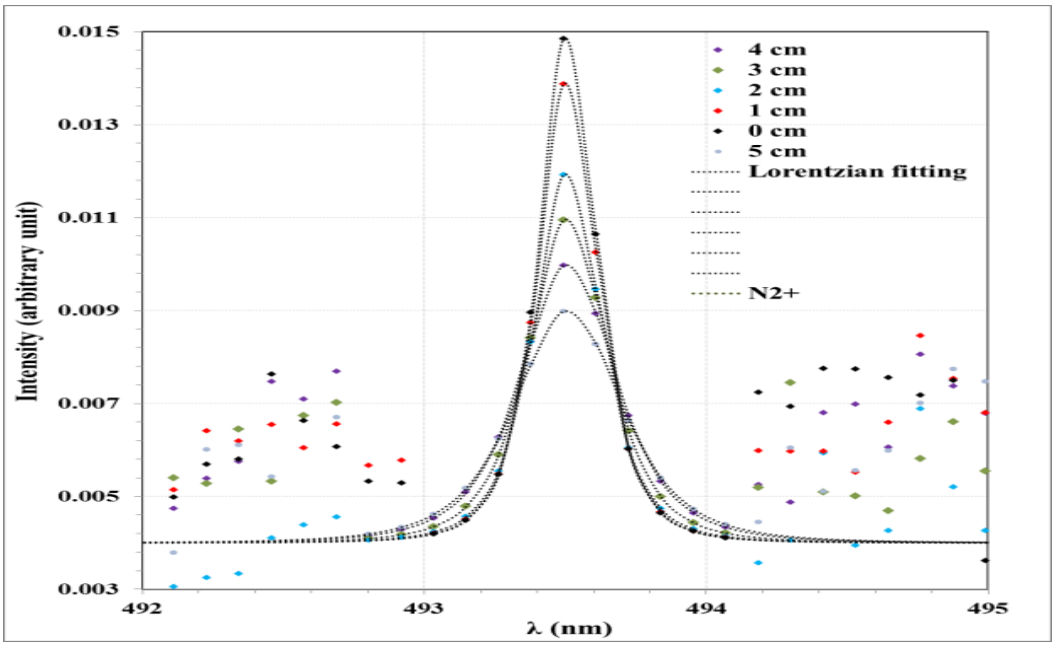

Figure 9- (493.5 nm) peaks broadening and Lorentzian fitting with different horizontal distance.

Figure 10 shows that the DBD plasma temperature is increasing with a decrease in the horizontal opposite surface area of the electrodes. The temperature increased from about 1.231 eV to 1.462 eV with the decrease in the electrodes horizontal surface area, due to the fact that the electric resistance of external circuit decreases with the decrease in the horizontal surface area of the electrodes, which results in increase of the discharge voltage across the gap, accordingly, the discharge across gap is also multiply.

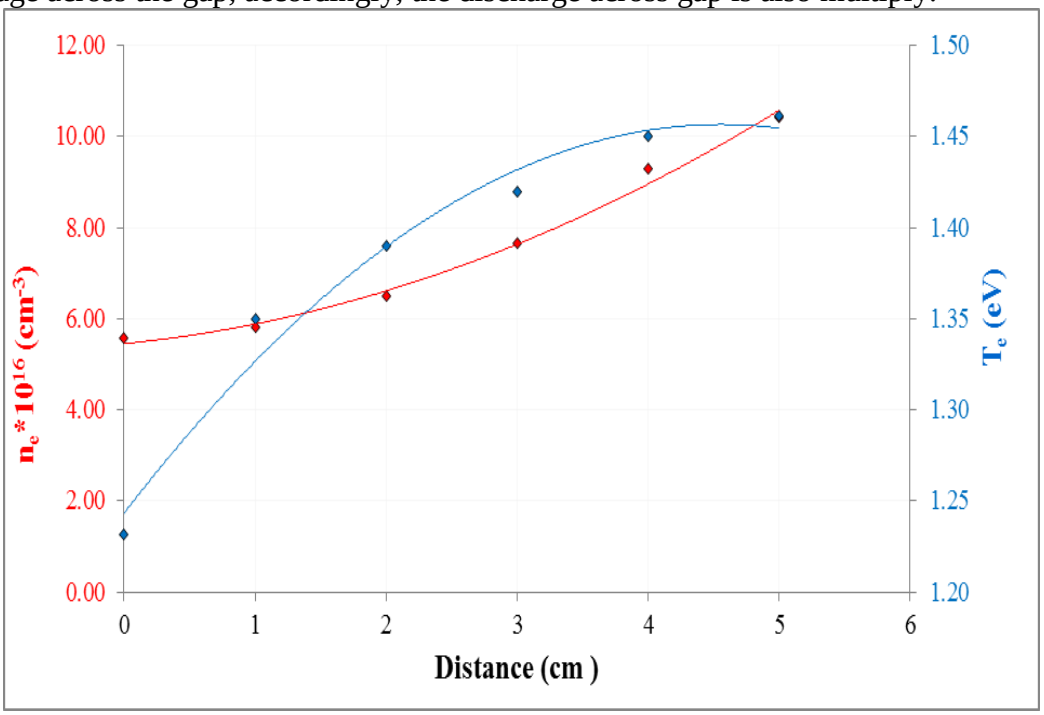

Figure 10-The variation of (T_e) and (n_e) versus decrease in the electrodes surface area

Table 1 presents the plasma parameters for pure epoxy with different distances in air (0cm-5cm), 0cm means no change in the matched surface area, i.e. completely matched, the electrode were moved away from each other to a distance of 5 cm. It can be noticed

that (f_P), (n_e) and (T_e) increased with the decrease in the electrodes surface area, but λ_D decreased in the same operating conditions. Through the results, it was noted that the values of N_D>>> 1 and is one of the conditions of the plasma.

Table 1- Plasma parameters in air for pure epoxy dielectric with different distances

Distance (cm)	Te (eV)	FWHM (nm)	$n_{e*}10^{16}$ (cm^{-3})	f_p*10^{12} (Hz)	λ_D*10^{-6}(cm)	N_D
0	1.231	0.240	5.551	2.116	3.499	10
1	1.349	0.250	5.782	2.159	3.589	11
2	1.390	0.280	6.476	2.285	3.442	11
3	1.419	0.330	7.633	2.481	3.203	11
4	1.450	0.400	9.252	2.731	2.941	10
5	1.461	0.450	10.408	2.897	2.783	9

The reducing of the distance between the electrodes is critical in the generation of plasma, where DBD plasma characteristics in air depend on the applied voltage as well as on the inter-electrode distance and the surface area. The increase of the applied voltage affects the properties of (DBD) plasma such as the electric field, electron density, and the concentration of active species[2].

3.2.2 With epoxy-copper dielectric

For more information about the DBD plasma temperature, the above measurements were repeated with epoxy-copper as the dielectric. The results showed the same behaviour as with epoxy, but the temperature generally was less. This is due to the difference in the dielectric constants which leads to energy decreases with the decrease in the permittivity of the material, as in Figure 11.

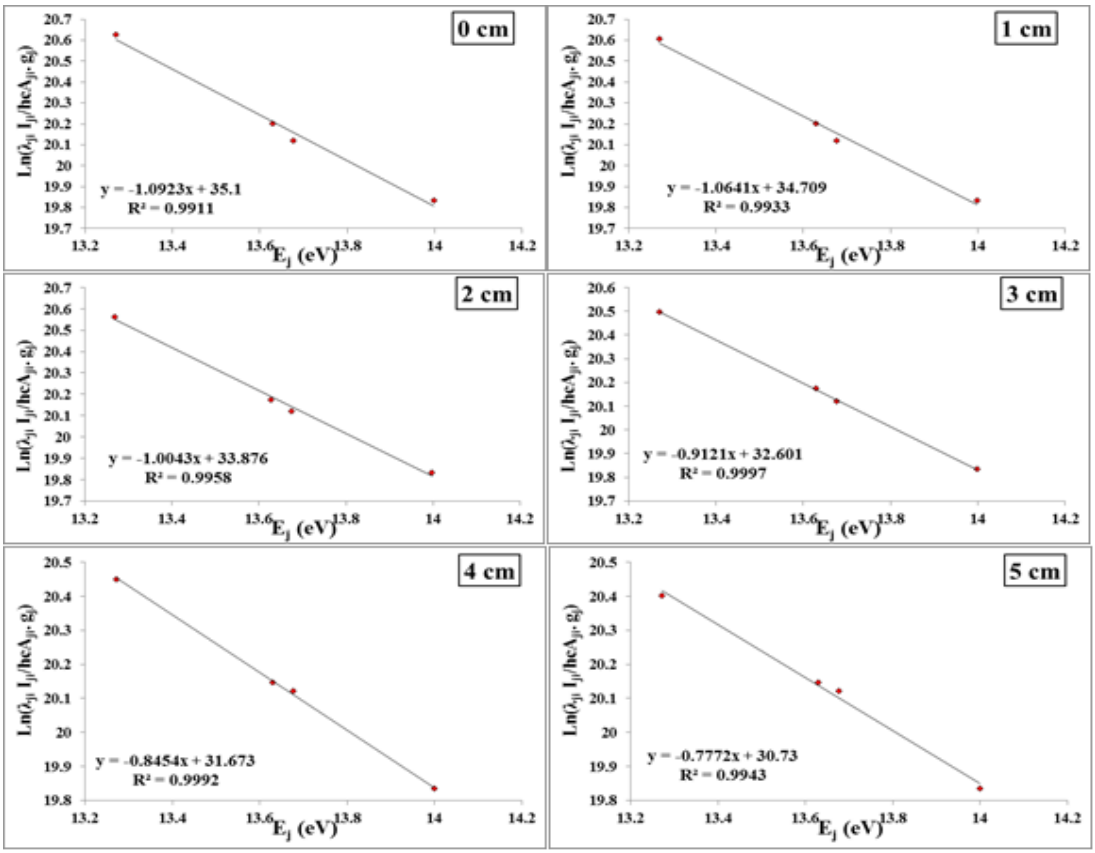

Figure 11-Boltzmann plots with epoxy-copper dielectric with different distances.

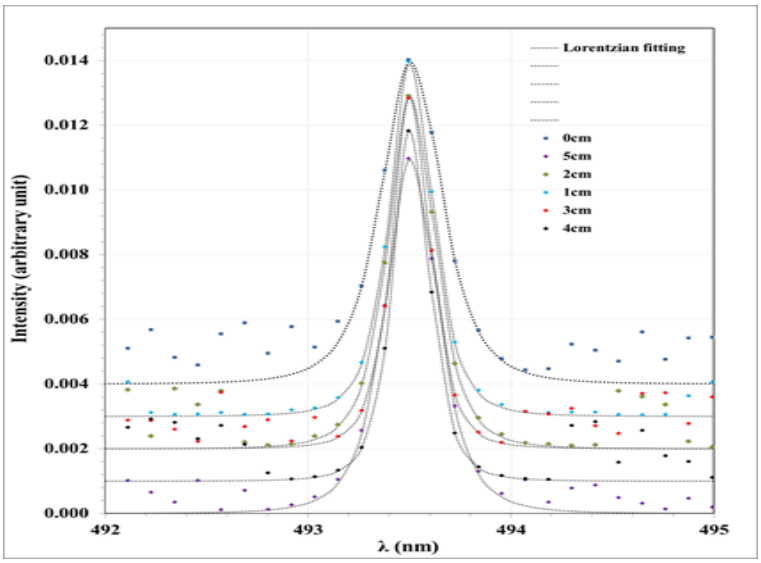

Figure 12-(493.5 nm) peaks broadening and Lorentzian fitting at different electrodes surface area.

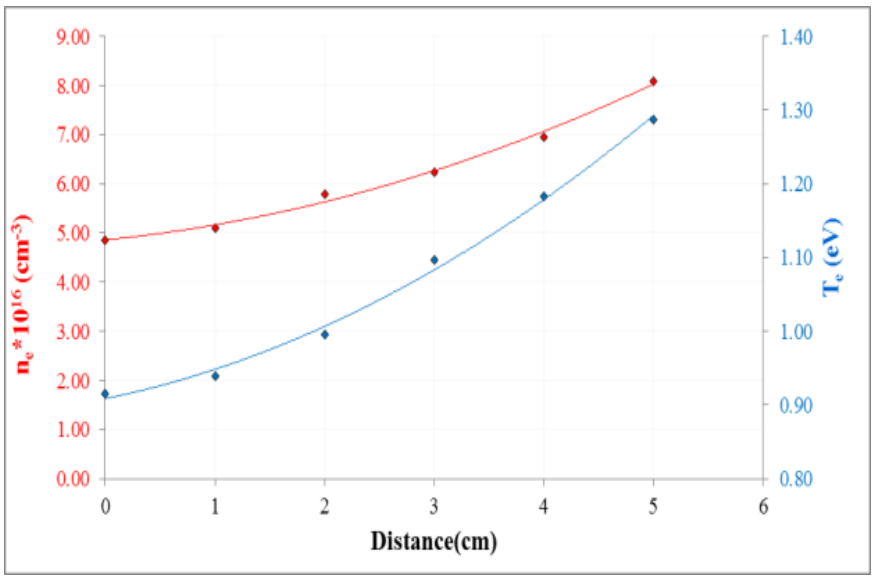

Figure 13-The variation of (T_e) and (n_e) versus the electrodes surface area.

Table 2- Plasma parameters for epoxy-copper dielectric with different distances in air

Distance (cm)	Te (eV)	FWHM (nm)	$n_{e*}10^{16}$ (cm^{-3})	f_p *10^{12} (Hz)	λ_D *10^{-6}(cm)	N_D
0	0.915	0.210	4.857	1.979	3.226	7
1	0.940	0.220	5.088	2.026	3.193	7
2	0.996	0.250	5.782	2.159	3.083	7
3	1.096	0.270	6.245	2.244	3.113	8
4	1.183	0.300	6.939	2.365	3.068	8
5	1.287	0.350	8.095	2.555	2.962	9

Conclusions

In this work, it was observed that there was a significant effect of the electrodes surface area and the type of insulator material on the properties of the generated plasma. The strength of discharge grew with the decrease of the electrodes surface area, which

led to the increase in the density of the plasma on the surface of the electrical insulator and thus the increase in the electrons temperature. These values vary from one insulator to another depending on the material's dielectric constant. The epoxy dielectric was higher than the epoxy/copper dielectric.

References

[1] E. Flaxer, "Real time controller for dielectric barrier discharge using DSP," in *2012 IEEE 27th Convention of Electrical and Electronics Engineers in Israel*, pp. 1–4, 2012.

[2] U. Kogelschatz, B. Eliasson, and W. Egli, "Dielectric-barrier discharges. Principle and applications," *Journal de Physique IV Proceedings, EDP Sciences*, vol. 7, no. C4, pp. 47-66, 1997.

[3] A. Chirokov, A. Gutsol, and A. Fridman, "Atmospheric pressure plasma of dielectric barrier discharges," *Pure Appl. Chem.*, vol. 77, no. 2, pp. 487–495, 2005.

[4] D. P. Subedi, U. M. Joshi, and C. S. Wong, "Dielectric barrier discharge (DBD) plasmas and their applications," in R. Rawat(eds) *Plasma Science and Technology for Emerging Economies*, Springer, pp. 693–737, 2017.

[5] M. Rubinstein and R. H. Colby, *Polymer physics*, vol. 23. Oxford university press New York, 2003.

[6] T. C. Corke, C. L. Enloe, and S. P. Wilkinson, "Dielectric barrier discharge plasma actuators for flow control," *Annu. Rev. Fluid Mech.*, vol. 42, pp. 505–529, 2010.

[7] E. Moreau, "Airflow control by non-thermal plasma actuators," *J. Phys. D.: Appl. Phys.*, vol. 40, no. 3, p. 605, 2007.

[8] R. Erfani, H. Zare-Behtash, and K. Kontis, "Influence of shock wave propagation on dielectric barrier discharge plasma actuator performance," *J. Phys. D.: Appl. Phys.*, vol. 45, no. 22, p. 225201, 2012.

[9] M. Forte, J. Jolibois, J. Pons, E. Moreau, G. Touchard, and M. Cazalens, "Optimization of a dielectric barrier discharge actuator by stationary and non-stationary measurements of the induced flow velocity: application to airflow control," *Exp. Fluids*, vol. 43, no. 6, pp. 917–928, 2007.

[10] R. Erfani, T. Erfani, S. V Utyuzhnikov, and K. Kontis, "Optimisation of multiple encapsulated electrode plasma actuator," *Aerosp. Sci. Technol.*, vol. 26, no. 1, pp. 120–127, 2013.

[11] D. Hegemann, H. Brunner, and C. Oehr, "Plasma treatment of polymers for surface and adhesion improvement," *Nucl. instruments methods Phys. Res. Sect. B Beam Interact. with Mater. atoms*, vol. 208, pp. 281–286, 2003.

[12] S. H. Saleh, I. H. Hashim, and K. A. Aadim, "Effect of Electrodes types on the Properties of the Dielectric Barrier Discharge Plasma," *Journal of College Education,.*, vol. 20, no. 3, pp. 151–158, 2019.

[13] D. Tețoi, D. E. Crețu, O. Beniugă, R. Burlică, D. Astanei, and M. Olariu, "DBD Plasma in Air Reactor for Polymeric Surfaces Treatment," in *2020 International Conference and Exposition on Electrical And Power Engineering (EPE)*, pp. 636–639, 2020.

[14] A. M. Farhan, N. J. Kadhim, and H. I. Jaafer, "Theoretical Study of EUXIT 50 KI Epoxy and its Hardener using Hyperchem-8 Program," *Asian Journal of Applied Science and Engineering*, vol. 5, no. 3, p. 159, 2014.

[15] S. B. Bayram and M. V Freamat, "Vibrational spectra of N2: An advanced undergraduate laboratory in atomic and molecular spectroscopy," *Am. J. Phys.*, vol. 80, no. 8, pp. 664–669, 2012.

[16] W. T. Y. Mohamed, "Fast LIBS identification of aluminum alloys," *Prog. Phys.*, vol. 2, pp. 87–92, 2007.

[17] N. Konjević, A. Lesage, J. R. Fuhr, and W. L. Wiese, "Experimental Stark widths and shifts for spectral lines of neutral and ionized atoms (a critical review of selected data for the period 1989 through 2000)," *J. Phys. Chem. Ref. Data*, vol. 31, no. 3, pp. 819–927, 2002.